Controlling charge injection by self-assembled monolayers in bottom-gate and top-gate organic field-effect transistors

Gholamrezaie, Fatemeh; Asadi, Kamal; Kicken, Romero A. H. J.; Langeveld-Voss, Bea M. W.; de Leeuw, Dago M.; Blom, Paul W. M.

Published in:
Synthetic Metals

DOI:
10.1016/j.synthmet.2011.08.020

Synthetic Metals 161 (2011) 2226–2229

Contents lists available at ScienceDirect

Synthetic Metals

journal homepage: www.elsevier.com/locate/synmet

Controlling charge injection by self-assembled monolayers in bottom-gate and top-gate organic field-effect transistors☆

Fatemeh Gholamrezaie[a,*], Kamal Asadi[a], Romero A.H.J. Kicken[b], Bea M.W. Langeveld-Voss[b], Dago M. de Leeuw[a,c], Paul W.M. Blom[a,d]

[a] Molecular Electronics, Zernike Institute for Advanced Materials, University of Groningen, 9747 AG, Groningen, The Netherlands
[b] TNO Science & Industry, Dept. Multilayer Devices, De Rondom 1, 5600 HE, Eindhoven, The Netherlands
[c] Philips Research Laboratories, High Tech Campus 4, 5656 AA, Eindhoven, The Netherlands
[d] TNO/Holst Centre, High Tech Campus 31, 5605 KN, Eindhoven, The Netherlands

ARTICLE INFO

Article history:
Received 31 May 2011
Received in revised form 2 August 2011
Accepted 9 August 2011
Available online 25 September 2011

Keywords:
Charge injection
Self-assembled monolayer
Organic field-effect transistor

ABSTRACT

We investigate the modulation of the charge injection in organic field-effect transistors with self-assembled monolayers (SAMs) using both a bottom-gate and a top-gate geometry. The current modulation by using SAMs is more pronounced in the top-gate geometry due to the better defined upper surface of the bottom source and drain electrodes. By modifying Ag electrodes with a perfluorinated monolayer an injection barrier as high as 1.6 eV into poly(9,9-dioctylfluorene) can be surmounted, enabling the measurement of the saturated field-effect mobility of 6×10^{-5} cm^2 V^{-1} s^{-1}.

1. Introduction

In recent years organic materials, and especially conjugated polymers, have attracted considerable attention for application in polymeric and molecular electronic devices because of their unique mechanical and electrical properties. The solution processability provides the opportunity to produce on large area plastic substrates low-cost devices such as pixel engines in large-area active matrix displays and circuit components in radio frequency identification tags or smart cards [1]. The use of conjugated polymers in field-effect transistors (OFET) [2] and integrated circuits [3] requires a precise control of the key device parameters such as mobility, current modulation and threshold voltage. The device mobility of OFETs [4] depends, apart from sample preparation and deposition methods [1,3,5,6], on charge injection and transport [7]. The charge transport mechanism in OFETs is well-established [8,9], whereas the physical understanding of charge injection is less developed [10].

The hole injection in organic electronic devices is affected by the energy difference between the Fermi level of the metal electrodes and the energy of highest occupied molecular orbital (HOMO) of the polymeric semiconductor [11,12]. Lowering this energy difference will improve the charge injection [13–15]. The injection barrier for a given polymer can be controllably tuned by changing the work function of the electrode through the use of self-assembled monolayers (SAMs). Alkanethiols are well-known to self-assemble into dense and uniform monolayers on metals like Au, Ag, Cu, Hg, and Pd. The macroscopic electric dipole moment of the ordered monolayer leads to a charge redistribution of the metal surface. The work function of the metal/SAM system is therefore substantially different than that of the bare metal [16–18].

SAMs have been used to modify the work function of source and drain electrodes, especially in FETs based on polycrystalline semiconductors like pentacene [19–24]. However, in that case the reported changes in current modulation can, next to modulation of the injection barrier, also be due to different morphology of the deposited semiconductor at the contact. To unambiguously correlate a change in current modulation to a change in injection barrier due to application of a SAM, we apply amorphous semiconductors.

Beside injection barriers also the geometry of the OFET can have a large effect on the device mobility [25]. Three common geometries have been reported: the bottom contact/bottom-gate (BC/BG), bottom contact/top-gate (BC/TG) and top contact/bottom-gate (TC/BG) configuration, as shown in Fig. 1 [4]. The top contact/bottom-gate (TC/BG) is similar to an inverted bottom contact/top-gate (BC/TG) and therefore disregarded. The difference between the bottom gate and top gate configuration is the position of the source and drain electrode with respect to both the gate electrode and the transport channel. In the bottom gate configuration, charges are

☆ Dedicated to the memory of Prof. Bert de Boer who passed away in January 2009.

* Corresponding author. Tel.: +31 40 2742547.
E-mail address: fatemeh.gholamrezaie@philips.com (F. Gholamrezaie).

0379-6779/$ – see front matter © 2011 Elsevier B.V. All rights reserved.
doi:10.1016/j.synthmet.2011.08.020

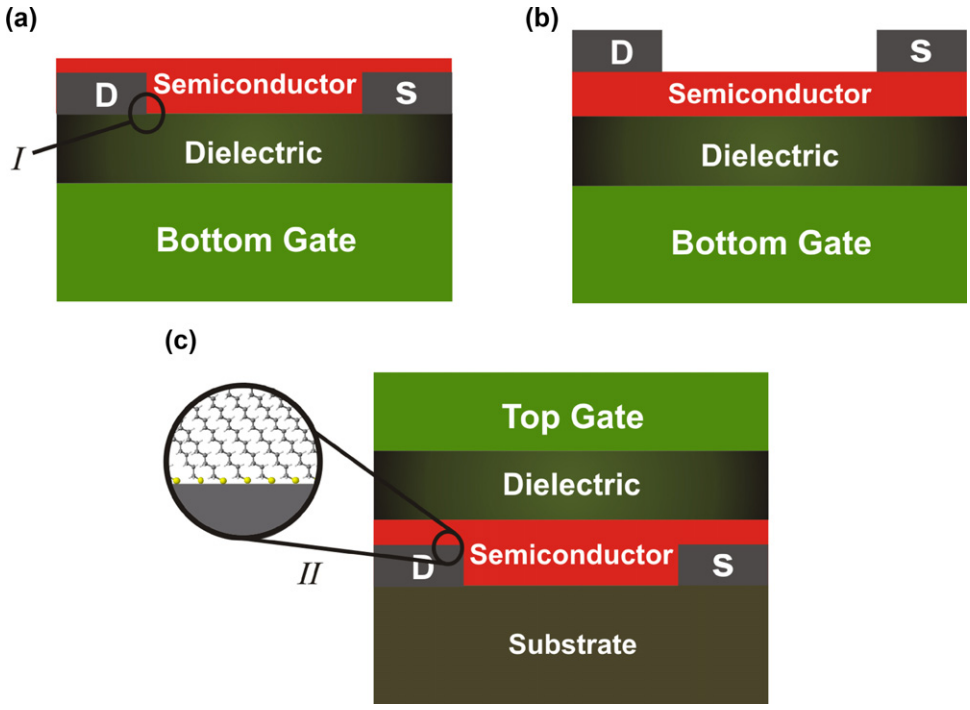

Fig. 1. Field-effect transistors configurations: (a) bottom contact, bottom gate (BC/BG); (b) top contact, bottom gate (TC/BG); (c) bottom contact, top gate (BC/TG). The injection area at the ill-defined corner of the metal electrode in the bottom gate configuration (*I*) and the perpendicular injection area at the metal electrode in the top gate configuration (*II*) are highlighted.

directly injected from the electrode into the transport channel at the semiconductor/gate dielectric interface. In the top gate configuration the source and drain electrode are separated from the transport channel by a bulk semiconductor layer. The charges are then injected not only from the edge of the electrodes but also from those parts of the electrode that overlap with the gate: the upper surface area of the electrodes [26–29]. The question is now whether a modification of the workfunction of the source and drain electrode by SAMs is equally effective in the different configurations. Here, we report the effect of modifying the injecting bottom contacts using SAMs in the bottom-gate and top-gate geometry.

2. Experimental

Organic field-effect transistors were made using heavily doped silicon wafers as bottom-gate electrode, with a 250 nm thick layer of thermally grown SiO_2 as a bottom-gate dielectric. 80 nm Ag source and drain electrodes were defined by photolithography on a 2 nm Cr adhesion layer. Two SAMs were investigated, hexadecanethiol (HDT) and 1H,1H,2H,2H-perfluorodecanethiol (PFDT). The substrates with Ag electrodes were immersed for two days into the ethanolic solution of the molecules of about $1–3 \times 10^{-3}$ M. After self-assembly, the substrates were thoroughly rinsed with ethanol, toluene, and 2-propanol, and dried with a deionized N_2 flow. Prior to the deposition of the organic semiconductor the substrate was treated with HMDS to passivate the surface. The semiconducting polymers poly(2-methoxy-5-(2′-ethylhexyloxy)-1,4-phenylene vinylene) (MEH-PPV) and poly(9,9-dioctylfluorene) (PFO) were spincoated from toluene in a glove box. The layer thickness was around 50 nm for MEH-PPV and 80 nm for PFO. A 400 nm layer of poly(trifluoro-ethylene) (PTrFE) was used as a top-gate dielectric. The transistor was finished by evaporation through a shadow mask of 80 nm Ag as the top-gate. Electrical measurements were carried out in a probe station under high vacuum (10^{-6} mbar) with a Keithley 4200–SCS Semiconductor Characterization System. The electrical characteristics are measured for both the top-gate transistor and the bottom-gate transistor processed on the same wafer.

3. Results and discussion

The dipole moment of SAMs of alkanethiols and perfluorinated-alkanethiols exhibit a different sign [13,16]. Therefore they either increase or decrease the workfunction. The work function of Ag as measured with a Kelvin probe amounted to 4.3 eV. Application of a HDT SAM yields a workfunction of 3.8 eV and application of a PFDT SAM yields a workfunction of 5.5 eV. The values derived here are comparable to the values as measured and calculated in earlier work [16,30].

The output characteristics of bottom-gate transistors with MEH-PPV as the semiconductor (chemical structure as inset) and bare and SAM modified source and drain electrodes are presented in Fig. 2a. We observe that the current modulation using bare Ag electrodes is rather poor. The current modulation does not change using HDT modified electrodes. A small increase however is observed when using PFDT modified electrodes. The output characteristics of the corresponding bottom-gate transistors are presented in Fig. 2b. The current modulation is poor with bare Ag electrodes and even decreases using HDT treated electrodes. However, an enhanced current modulation is observed using PFDT modified electrodes. We note that the current enhancement using PFDT is larger in the top-gate configuration than in the bottom-gate configuration.

The differences in current modulation correspond with the changes in injection barrier. The HOMO of MEH-PPV is situated at 5.2 eV. Hence the injection barriers are estimated as 0.9 eV for bare Ag electrodes, 1.4 eV for HDT modified electrodes and −0.3 eV for using PFDT modified electrodes. The current in the transistors with bare Ag electrodes is injection limited. The injection is worse using HDT modified electrodes and improves using PFDT modified electrodes. The current enhancement in the top-gate transistor is generally larger compared the bottom-gate configuration due to lower contact resistances [31]. Regardless of the FET configuration,

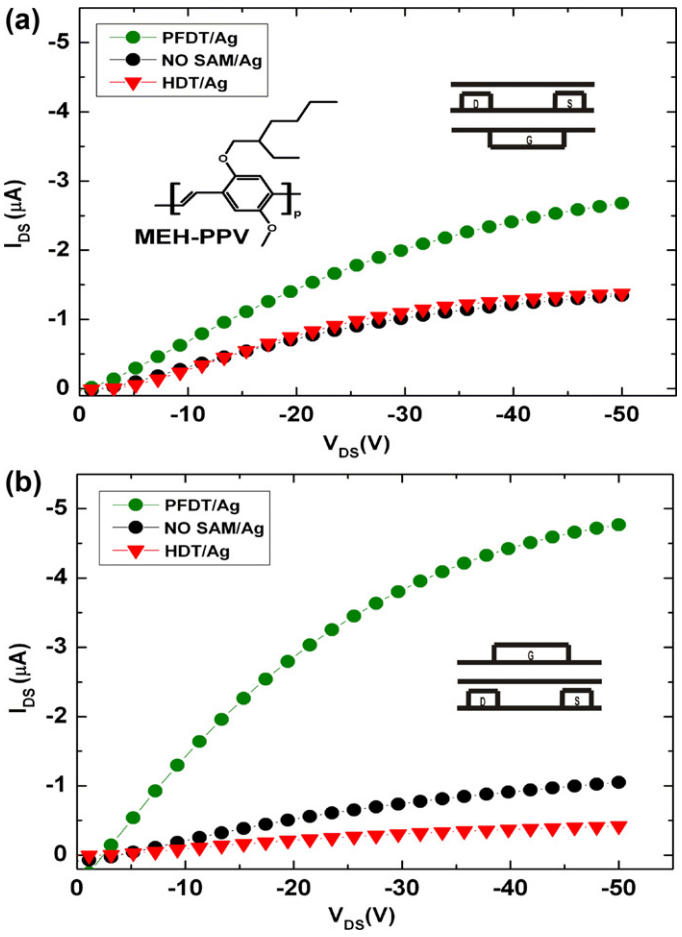

Fig. 2. Output characteristics of a MEH-PPV bottom-gate field-effect transistor (a) and of a top-gate field-effect transistor (b). Black circles represent bare Ag source-drain electrodes; red triangles HDT modified Ag electrodes and green circles PFDT modified Ag electrodes. The channel widths and channel lengths are 20 mm and 20 μm. The gate bias is −50 V. The inset shows the chemical structure of MEH-PPV. (For interpretation of the references to color in this figure legend, the reader is referred to the web version of the article.)

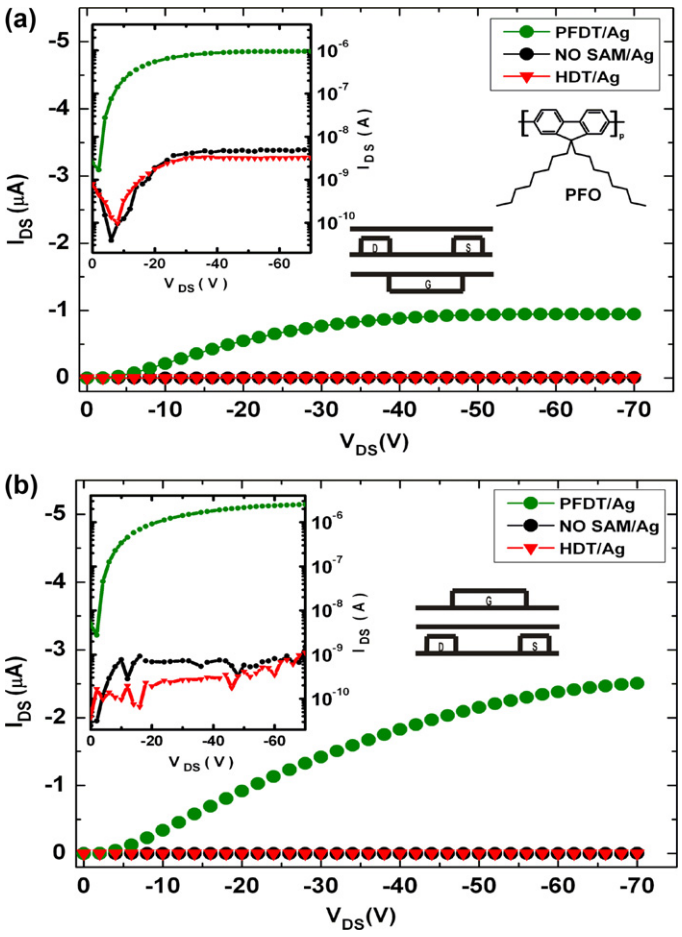

Fig. 3. Output characteristics of a PFO bottom-gate field-effect transistor (a) and of a top-gate field-effect transistor (b). Black circles represent bare Ag source-drain electrodes; red triangles HDT modified Ag electrodes and green circles PFDT modified Ag electrodes. The insets present the current on a semi-logarithmic scale. The channel widths and channel lengths are 10 mm and 20 μm. The gate bias is −40 V. The inset shows the chemical structure of PFO. (For interpretation of the references to color in this figure legend, the reader is referred to the web version of the article.)

both SAM layer affect the performance. PFDT increases the current in the output characteristics of the MEH-PPV OFET whereas HDT lowers the current output. However, the influence of both HDT and PFDT SAMs on charge injection in top-gate configuration is more pronounced than the bottom-gate. We attribute these differences to the quality of the SAM. In bottom-gate OFET, the conducting channel is directly in contact with the source and drain electrodes. The conducting channel in OFETs has been proven to be in the order of a few nanometers [32–34]. The rest of the semiconductor actually does not participate in the transport. Charge injection in OFETs therefore takes places in very narrow region namely the corner of the electrode/dielectric interface as depicted with (*I*) in Fig. 1a. The side indicated with (*I*) of the deposited metal electrode may have an ill-defined crystal structure, and not clearly Ag(1 1 1) [35]. Highly ordered thiol SAMs however are formed on well-defined metallic surfaces such as Ag(1 1 1) [16]. Due to ill-defined crystal structure at the corner of the electrode with the semiconductor/gate dielectric the monolayer is expected to be highly disordered. Subsequently the workfunction does not correspond to that measured for modified bulk electrodes i.e. Ag(1 1 1). The injection barrier in the corner therefore is larger than expected from the Kelvin probe measurement [36–40]. Measuring the actual value of the work function however is hampered by experimental limitations. In the top-gate geometry however the whole top surface, Ag(1 1 1) of the electrode that overlaps with the gate electrode is injecting. The Kelvin probe measurement shows that the SAM is macroscopically ordered as pointed in Fig. 1c [41]. Hence the injection barrier in the top-gate configuration is effectively lowered and the current is enhanced.

In order to estimate the injection barrier that can be surmounted by a SAM we used a semiconducting polymer with a deeper lying HOMO, *viz.* PFO, the chemical structure of which is shown as inset in Fig. 3a. The HOMO of PFO is located at 5.9 eV leading to an injection barrier with bare Ag of 1.6 eV. The output characteristics of bottom-gate transistors using both bare and SAM modified source and drain electrodes are presented in Fig. 3a. As inset, the current modulation by applying SAMs is shown on a logarithmic scale. When using bare Ag or HDT modified electrodes, there is no current modulation. The injection is completely blocked due to the large injection barriers estimated as 1.6 eV and 2.1 eV respectively. Only when using PFDT modified electrodes charge can be injected and current modulation is observed, which agrees with the estimated small injection barrier of only 0.4 eV.

The output curves of the corresponding PFO top-gate transistors are presented on a linear scale in Fig. 3b. For comparison the inset shows the output curves on a semi-logarithmic scale. Similarly as in Fig. 3a, when using either bare Ag or HDT modified electrodes there is no charge injection and no current modulation. With PFDT modified electrodes current modulation is observed, which indicates that the use of SAMs can surmount an injection barrier of 1.6 eV. The current in the top-gate configuration is slightly larger

than that in the bottom gate configuration. The saturated device mobility is calculated as $6 \times 10^{-5}\,cm^2\,V^{-1}\,s^{-1}$. The slightly larger device mobility in the top gate configuration as compared to the bottom configuration can be due to the microscopic order in the SAM, as explained above for the MEH-PPV transistors.

4. Conclusion

In summary, the injection barrier in field-effect transistors can be tuned by using SAM modified source and drain electrodes. We have demonstrated that barriers up to 1.6 eV can be surmounted. For such barrier hardly any FET characteristics is observed for bare electrodes. The modification is more effective in a top-gate configuration than in a bottom-gate configuration, which is due to a better order of the molecules in the SAM on top of the electrodes as compared to the side and corner of the electrode.

Acknowledgements

We gratefully acknowledge technical support of J. Harkema and financial support from the research program of the Dutch Polymer Institute (DPI) Project no. 624, and the EU project ONE-P no. 212311.

References

[1] C.D. Dimitrakopoulos, P.R.L. Malenfant, Adv. Mater. 14 (2002) 99.
[2] B. Crone, A. Dodabalapur, Y.-Y. Lin, R.W. Filas, Z. Bao, A. LaDuca, R. Sarpeshkar, H.E. Katz, W. Li, Nature 403 (2000) 521.
[3] H. Sirringhaus, N. Tessler, R.H. Friend, Science 280 (1998) 1741.
[4] P.V. Necliudov, M.S. Shur, D.J. Gundlach, T.N. Jackson, J. Appl. Phys. 88 (2000) 6594.
[5] D.M. DeLongchamp, S. Sambasivan, D.A. Fischer, E.K. Lin, P. Chang, A.R. Murphy, J.M. Fréchet, V. Subramanian, Adv. Mater. 17 (2005) 2340.
[6] A.R. Murphy, J.M.J. Fréchet, Chem. Rev. 107 (2007) 1066.
[7] L. Bürgi, T.J. Richards, R.H. Friend, H. Sirringhaus, J. Appl. Phys. 94 (2003) 6129.
[8] (a) C. Tanase, E.J. Meijer, P.W.M. Blom, D.M. de Leeuw, Phys. Rev. Lett. 91 (2003) 216601;
(b) M.C.J.M. Vissenberg, M. Matters, Phys. Rev. B 57 (1998) 12964;
(c) W.F. Pasveer, J. Cottaar, C. Tanase, R. Coehoorn, P.A. Bobbert, P.W.M. Blom, D.M. de Leeuw, M.A.J. Michels, Phys. Rev. Lett. 94 (2005) 206601.
[9] H. Sirringhaus, Adv. Mater. 17 (2005) 2411.
[10] T. van Woudenbergh, P.W.M. Blom, M.C.J.M. Vissenberg, J.N. Huiberts, Appl. Phys. Lett. 79 (2001) 1697.
[11] G. Horowitz, P. Lang, M. Mottaghi, H. Aubin, Adv. Funct. Mater. 14 (2004) 1069.
[12] N. Koch, ChemPhysChem 8 (2007) 1438.
[13] K. Asadi, F. Gholamrezaie, E.C.P. Smits, P.W.M. Blom, B. de Boer, J. Mater. Chem. 17 (2007) 1947.
[14] (a) I.H. Campbell, J.D. Kress, R.L. Martin, D.L. Smith, N.N. Barashkov, J.P. Ferraris, Appl. Phys. Lett. 71 (1997) 3528;
(b) S. Khodabakhsh, D. Poplavskyy, S. Heutz, J. Nelson, D.D.C. Bradley, H. Murata, T.S. Jones, Adv. Funct. Mater. 14 (2004) 1205.
[15] B.H. Hamadani, D.A. Corley, J.W. Ciszek, J.M. Tour, D. Natelson, Nano Lett. 6 (2006) 1303.
[16] B. de Boer, A. Hadipour, M.M. Mandoc, T. van Woudenbergh, P.W.M. Blom, Adv. Mater. 17 (2005) 621.
[17] I.H. Cambell, S. Rubin, T.A. Zawodzinski, J.D. Kress, R.L. Martin, D.L. Smith, N.N. Barashkov, J.P. Ferraris, Phys. Rev. B 554 (1996) 14321.
[18] R.W. Zehner, B.F. Parsons, R.P. Hsung, L.R. Sita, Langmuir 15 (1999) 1121.
[19] Z. Jia, V.W. Lee, I. Kymissis, L. Floreano, A. Verdini, A. Cossaro, A. Morgante, Phys. Rev. B 82 (2010) 125457.
[20] D. Boudinet, M. Benwadih, Y. Qi, S. Altazin, J. Verilhac, M. Kroger, C. Serbutoviez, R. Gwoziecki, R. Coppard, G. Le Blevennec, A. Kahn, G. Horowitz, Org. Electron. 11 (2010) 227.
[21] D. Yun, S.W. Rhee, J. Mater. Chem. 20 (2010) 9754.
[22] K. Asadi, Y. Wu, F. Gholamrezaie, P. Rudolf, P.W.M. Blom, Adv. Mater. 21 (2009) 4109.
[23] J. Hong, A. Park, S. Lee, J. Kang, N. Shin, D.Y. Yoon, Appl. Phys. Lett. 92 (2008) 143311.
[24] P. Marmont, N. Battaglini, P. Lang, G. Horowitz, J. Hwang, A. Kahn, C. Amato, P. Calas, Org. Electron. 9 (2008) 419.
[25] Y. Roichman, N. Tessler, Appl. Phys. Lett. 80 (2002) 151.
[26] I.G. Hill, Appl. Phys. Lett. 87 (2005) 163505.
[27] T.J. Richards, H. Sirringhaus, J. Appl. Phys. 102 (2007) 094510.
[28] T. van Woudenbergh, J. Wildeman, P.W.M. Blom, J.J.A.M. Bastiaansen, B.M.W. Langeveld-Voss, Adv. Funct. Mater. 14 (2004) 667.
[29] C. Chiang, S. Martin, J. Kanicki, Y. Ugai, T. Yukawa, S. Takeuchi, Jpn. J. Appl. Phys. 37 (1998) 5914.
[30] S.G.J. Mathijssen, P.A. van Hal, T.J.M. van den Biggelaar, E.C.P. Smits, B. de Boer, M. Kemerink, R.A.J. Janssen, D.M. de Leeuw, Adv. Mater. 20 (2008) 2703.
[31] K.P. Puntambekar, P.V. Pesavento, C. Daniel Frisbiea, Appl. Phys. Lett. 83 (2003) 5539.
[32] B. Crone, A. Dodabalapur, A. Gelperin, L. Torsi, H.E. Katz, A.J. Lovinger, Z. Bao, Appl. Phys. Lett. 78 (2001) 2229.
[33] M. Mottaghi, G. Horowitz, Org. Electron. 7 (2006) 528.
[34] M.A. Alam, A. Dodabalapur, M.R. Pinto, IEEE Trans. Electron. Dev. 44 (1997) 1332.
[35] N.A. Pangarov, Electrochim. Acta 7 (1962) 139.
[36] E. Orgiu, N. Crivillers, J. Rotzler, M. Mayor, P. Samorı, J. Mater. Chem. 20 (2010) 10798.
[37] A. Kahn, N. Koch, W. Gao, Polym. Sci. B: Polym. Phys. 41 (2003) 2529.
[38] D.M. Alloway, M. Hofmann, D.L. Smith, N.E. Gruhn, A.L. Graham, R. Colorado, V.H. Wycoski, T.R. Lee, P.A. Lee, N.R. Armstrong, J. Phys. Chem. B 107 (2003) 11690.
[39] G. Ashkenasy, D. Cahen, R. Cohen, A. Shanzer, A. Vilan, Acc. Chem. Res. 35 (2002) 121.
[40] A. Vilan, D. Cahen, Trend Biotechnol. 20 (2002) 22.
[41] E. Ito, T. Arai, M. Hara, J. Noh, Bull. Korean Chem. Soc. 30 (2009) 1309.